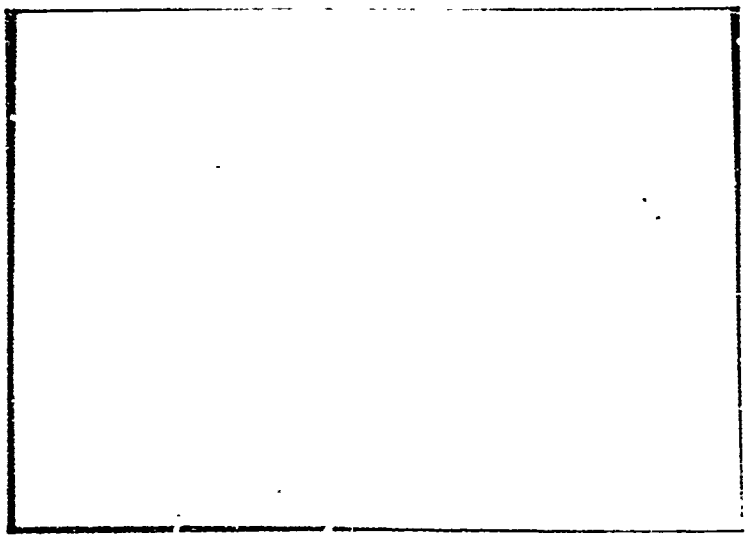

DEPARTMENT OF PHYSICS
UNIVERSITY OF SAN FRANCISCO

UNCLASSIFIED
Security Classification

DOCUMENT CONTROL DATA - R & D

(Security classification of title, body of abstract and indexing annotation must be entered when the overall report is classified)

1. ORIGINATING ACTIVITY (Corporate author)

University of San Francisco
San Francisco, California

2a. REPORT SECURITY CLASSIFICATION
UNCLASSIFIED

2b. GROUP

3. REPORT TITLE

Development of A High Energy Neutron Detector

4. DESCRIPTIVE NOTES (Type of report and inclusive dates)

Final Report

5. AUTHOR(S) (First name, middle initial, last name)

Dr. Eugene V. Benton
Dr. Alvin L. Frank

6. REPORT DATE	7a. TOTAL NO. OF PAGES	7b. NO. OF REFS
June 15, 1972		12

8a. CONTRACT OR GRANT NO.	9a. ORIGINATOR'S REPORT NUMBER(S)
b. PROJECT NO. NWET J11AAXP	DNA 2918F
c. Task and Subtask: X244	9b. OTHER REPORT NO(S) (Any other numbers that may be assigned this report)
d. Work Unit: 02	

10. DISTRIBUTION STATEMENT

Approved for public release;
distribution unlimited

11. SUPPLEMENTARY NOTES	12. SPONSORING MILITARY ACTIVITY
	Director Defense Nuclear Agency Washington, D. C. 20305

13. ABSTRACT

A detector is being developed for the measurement of high energy neutron fluences. A series of neutron energy thresholds are employed to yield spectral information. The method employed is to measure the fluences of elastically scattered recoil nuclei from low Z ($4<Z<8$) materials. Nuclear track recorders are used for this purpose. A cellulose nitrate track recorder which selectively registers recoil nuclei in the presence of ^4He- particle backgrounds has been developed. Neutron energy thresholds are due to selected thicknesses of gold degrader films which separate the recoil particle radiator and the track recorder. The detector will be applicable to the measurement of neutrons in the energy range of 5 to 20 MeV. The present methods of track density readout, the useful fluence range will be approximately 1.5×10^8 to 5×10^{11} neutrons/cm^2. A computer code (FLUENZ) has been written to supplement detector response measurements and to determine response over the full useful neutron energy range. Another computer code (HENDU) is being adapted to the unfolding of neutron spectra from the detector measurements.

DD FORM 1 NOV 65 1473 (PAGE 1)

S/N 0101-807-6801

UNCLASSIFIED
Security Classification

14. KEY WORDS	LINK A		LINK B		LINK C	
	ROLE	WT	ROLE	WT	ROLE	WT
Neutron detector						
Neutron threshold detector						
Track information						

UNIVERSITY OF SAN FRANCISCO
SAN FRANCISCO, CALIFORNIA 94117

DNA NUMBER 2918F

DEVELOPMENT OF A HIGH ENERGY NEUTRON DETECTOR

This work has supported by the Defense Nuclear Agency under NWET subtask J11AAPX244-02

A. L. Frank and Dr. Eugene V. Benton

Final Report

Approved for public release; distribution unlimited.

Prepared under
Contract DASA 01-71-C-0065
for the
Defense Nuclear Agency

June 15, 1972

Contents

List of Illustrations

I. Introduction

Situations exist where it is necessary to measure the fluence and the energy spectra of high energy neutrons, $E_n \geq 5$ MeV. At the present time, the various methods developed to do this all have several limitations associated with their use. The highest energy threshold, found in the commonly used threshold detectors, is approximately 3 MeV for ^{32}S. The current state-of-the-art as well as the limitations of activation foil spectrometry have recently been described by McElroy[1] and Barrall.[2] It is pointed out that: 1) activation rate measurements, 2) fission yield errors, 3) evaluated cross section errors, and 4) errors associated with spectral unfolding procedure may combine to produce disagreements of up to 30% in fission spectra measurements as compared with other methods of analysis. The short half-life of some of the reactions is yet another limiting factor. Organic scintillation spectrometers are able to detect neutrons with superior efficiency and their output can be unfolded into neutron spectra. However, the spectrometers are not convenient for use in many situations. Their size, weight, and power requirements are a limitation. Also, there are still problems in spectra unfolding techniques, particularly at high energies.

One of the more significant new developments in the field of neutron detection has been made possible by the discovery of a new class of charged particle detectors called nuclear track detectors. The detecting principle is based on the delineation of individual paths of heavily ionizing charged particles such as fission fragments, recoil nuclei, alpha particles, and low velocity protons. Delineation is accomplished through a selective

chemical attack of the narrow, radiation damaged region along the particle's trajectory. The resulting narrow channels, referred to as tracks, can be enlarged to a convenient size for direct viewing with an optical microscope. Automated systems for track counting are now commercially available.

A program is underway to develop a high energy neutron detector (HEND) system.[3] The development program consists of (1) designing and fabricating a series of neutron recoil particle detectors from a general knowledge of recoil interactions, energetic ion transmissions, and track registration characteristics of nuclear track detectors, (2) calculating the response of the individual detectors to neutrons covering their useable energy ranges, (3) verification of the calculated detector response by experimental measurements performed at several neutron energies, and (4) development of a computer program which will unfold the HEND measurements.

As mentioned in earlier reports, the detectors are composed of a sandwich arrangement which includes the following:

(1) a radiator, consisting of a flat sheet of a material containing an element whose nuclei are elastically scattered by neutrons and ejected from the sheet,

(2) a degrader, a thin film, usually of gold, which reduces the energies of recoil nuclei transmitted through it, and

(3) a nuclear track detector, a sheet of plastic capable of recording the tracks of the energetic recoil nuclei impinging upon it. The detectors have the practical advantage of being small ($\sim$ 5 cm^2 total area), light (several grams), stable, and independent of any reaction

half-lives. The useful neutron energy range is from ~ 5 to 20 MeV. At energies of 5 MeV and below track recording efficiencies are low. Above 20 Mev inelastic interactions begin to compete significantly with the elastic scattering process.

II. Detectors

The detectors are designed to perform as a series of threshold detectors. The particular neutron threshold energy depends on the mass of the recoil nucleus and the thickness of the degrader. For a particular element and foil type, and with no degrader, neutrons of some minimum energy will produce tracks in the plastic with very low efficiency. As neutron energy increases, recoil energy and range also increase. Therefore, efficiency, not considering the elastic scattering cross section, continuously increases with energy.

When a degrader is introduced between the radiator and the track recorder, recoils of low energy are stopped in the degrader while those of higher energy are slowed down. Thus a degrader of a given thickness will tend to shift the response of the detector to higher neutron energies by a given amount. In this manner a series of degrader thicknesses produces a series of neutron threshold energies.

If the radiator is thicker than the ranges of the recoil particles, then the efficiency of the detector will increase steeply with neutron energy until the elastic scattering cross section begins to drop significantly. However, a thin radiator produces a detector with a somewhat different energy response. When recoil particle ranges equal radiator thickness the response begins to round off. Efficiency falls considerably below the thick radiator case for higher neutron energies. Detectors of this type are useful in that they sample lower neutron energies better, in comparison to higher energies, than do the thick radiator types.

The detection and accurate counting of recoil particle track densities places stringent requirements upon the track recorder employed. For any given recoil nucleus, there is both an upper and lower level of track registration sensitivity which the recorder must satisfy. The lower level is imposed by the background problem. ^{4}He particles are produced copiously within the radiators and plastic track recorders which have been used. Some degrader materials tested--notably, aluminum--also have significant (n, ^{4}He) cross sections. In track recorders sensitive to ^{4}He particles, the track densities from this source can be greater than track densities due to recoil particles. Since the ranges of ^{4}He particles are also much greater, the only way these spurious tracks may be excluded is by using a track recorder which is insensitive to ^{4}He particles.

At the same time, the track recorders must be sensitive enough to register recoil particles of the full range of energies produced. Further, the latent tracks must etch out such that $V_T/V_G \gg 1$, where V_T = etch rate along the particle path in the track recorder, and V_G = bulk etch rate of the track recording material. If the above condition is not met, two significant things occur. First, track registration becomes a strong function of the angle of impingement of the particle on the track recorder. Detector sensitivity is impaired, angular dependence of the detector is increased, and mathematical handling of the problem becomes difficult. Second, the tracks which are recorded may be in poor microscopic relief, thus making track counting less reliable. This is especially troublesome for those particles with very short ranges, which includes a large portion of the recoil nuclei produced.

The quality of the etched surface of the track recorder must also be

considered. In many materials etch pits form during etching that are not caused by ionizing particles. These pits may be indistinguishable from short recoil tracks. Where accurate track counting is desired, such recorders are not adequate.

Irradiations with 14 MeV neutrons were made to test various detector components. Radiators of three different recoil particles ^{9}Be, ^{12}C and ^{16}O were used. Degraders were made of thin aluminum foil and gold films which had been vacuum evaporated on to the radiators. The track recorders were Lexan polycarbonate plastic. Lexan is a plastic in common use which is known to be insensitive to ^{4}He particles while recording the tracks of stopping ions such as ^{12}C and ^{16}O.

The detectors employing Lexan did not yield recoil track density measurements of the quality required for this application. The detection efficiency of the Lexan recorder to neutron induced ^{9}Be recoils was only ~35%. Beryllium metal radiators should emit detectable fluences of recoils of approximately three times that of ^{12}C recoil fluences emitted by graphite. This greater sensitivity of beryllium is due to three factors. First, the elastic scattering cross section is somewhat greater for ^{9}Be than for ^{12}C. Second, the lighter ^{9}Be nucleus carries away a greater fraction of the energy from a collision with a neutron. Third, the smaller the Z of a particle of given energy, the greater is its range in matter. Thus, the sensitive thickness of the radiator for recoil emission is greater for lighter particles. However, measurements showed that these advantages of a beryllium radiator were lost due to the insensitivity of the Lexan track recorder.

Experiments showed that ^{12}C and ^{16}O recoil nuclei were efficiently recorded by Lexan. Even here, however, accuracy of measurement was less

than desired. The etched surface of Lexan, although acceptable for many applications, did not prove satisfactory for counting of short recoil tracks. A substantial and somewhat nonuniform background of etch pits resulted from small surface imperfections.

A survey of commercial materials did not reveal a recorder with the various track recording characteristics required. It was subsequently experimentally found that some track recorders have inherent limitations in their ability to discriminate between ions of different Z. With careful measurements of ions near the registration threshold, it was found that, in Lexan, V_T/V_G increased very gradually with increasing dE/dX. In celluiose nitrate, V_T/V_G increased very rapidly with dE/dX once the registration threshold was reached. It is this second type of track recorder which is required to discriminate against ^{4}He particles while still recording ^{9}Be recoil nuclei with maximum efficiency.

Cellulose nitrate plastics of the usual (commercial) compositions are quite sensitive to ^{4}He particles of energies up to ∿3 MeV. However, it was found that the sensitivity may be varied by altering the kind and amount of plasticizers included.[4] Plastics low in plasticizer content tend to have poor, nonuniform etching properties. Also, the more volatile plasticizers tend to be lost from the surface if included above a certain level, during preparation of plastic sheets. A series of plastics of decreasing sensitivities was manufactured by loading them with successively greater amounts of relatively nonvolatile plasticizers. By irradiating the specimens with stopping ^{4}He particles, it was possible to select plastics whose sensitivities were just below that needed to record ^{4}He particles. By varying fabrication procedures, it was possible to arrive at a plastic recorder which also exhibited the desired surface characteristics.

An irradiation with 14 MeV neutrons was made to test the final material. It was found that ^{9}Be recoil nuclei were registered efficiently. Very short tracks were clearly developed and longer tracks etched out with very small cone angles. Also, the surface imperfections did not appear to be a hindrance to track counting.

A series of beryllium radiator-gold degrader units were then manufactured by a vacuum evaporation technique. Aluminum degraders were found not suitable. They were found to produce background tracks even in plastics which are insensitive to ^{4}He particles. These are very short recoil particle tracks. The track densities produced were considerably smaller than from any of the radiators used. However, they were large enough to raise the background level by a factor of $\sim$2.5. Where thick radiators were desired, gold was evaporated onto 0.010 in thick beryllium squares. A 1 cm square contained four different gold thicknesses. For thin radiators, a tantalum sheet of 0.010 in thickness was used as a backing. Beryllium films of 0.250 mg/cm^2 were evaporated on 1 cm squares. Gold was then evaporated onto the beryllium as before. Table 1 gives a list of the detector combinations. For neutron energies up to 20 MeV, any beryllium radiator over 1.9 mg/cm^2 is thick in the sense that recoils of the maximum possible energy have ranges less than this value.

TABLE 1

Beryllium and Gold Thicknesses
For Radiator-Degrader Combinations

Beryllium Thickness (mg/cm^2)	Gold Thickness (mg/cm^2)
1.9	0
	0.495
	0.997
	1.384
	1.656
	2.416
	2.880
	3.732
	4.19
	4.81
	5.41
	5.99
0.250	0
	0.288
	0.770
	1.070
	1.45
	1.92
	2.65
	3.12

III. Detector Response

A method has been developed for the calculation of recoil nuclei track densities per unit incident neutron fluence for the HEND system. The physical parameters of any given detector can be inputted to a computer program, FLUENZ, which yields response versus energy for a discrete grid of neutron energies. It is assumed that neutrons are incident normally on the face of the detectors.

The geometry of the system is shown in Figure 1 where the degrader is omitted. Since the neutrons are incident normally, the recoil fluence is symmetrical with respect to the scattering angle, θ. An annular volume increment at distance s from P is given by

$$dV = 2\pi s^2 \sin\theta \, ds \, d\theta. \tag{1}$$

The number of nuclei in the volume increment is then given by

$$dN = 6.025 \times 10^{23} \times \rho \times \frac{dV}{A}, \tag{2}$$

where ρ is the density of the radiator material. If the radiator is not a single element and isotope, each nuclear component which contributes to recoil fluence must be calculated separately. The proper fractional density of the isotope is substituted into Equation 2 for ρ. The total elastic cross sectional area, in cm^2, of nuclei within the volume increment for a monoenergetic neutron beam is then given by

$$d\Sigma = dN \times \sigma \times 10^{-24}$$

$$d\Sigma = 0.6025\rho \, \sigma \frac{dV}{A}, \tag{3}$$

where σ, the elastic scattering cross section, is given in barns. Therefore, the number of elastic collisions in the volume increment per incident neutron/cm^2 is

$$dC = 0.6025\rho \, \sigma \frac{dV}{A}, \tag{4}$$

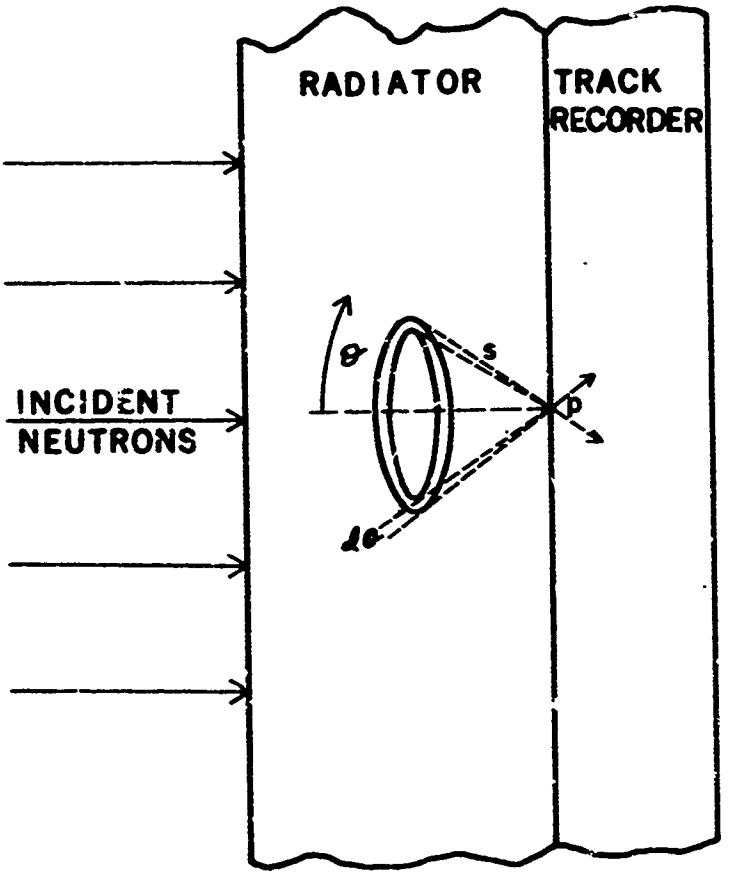

Figure 1

when the total attenuation of the neutron beam in the radiator is assumed to be negligible.

When an elastic collision takes place, the probability of a recoil emission per steradian at angle θ is assumed to be proportional to $\cos\theta$ at all neutron energies. In fact, there is some structure in the angular scattering probabilities for discrete neutron energies. However, these calculations were made for the average response of a detector for 0.5 MeV wide energy intervals. For the neutron energy region up to 20 MeV, the angular structure was expected to average out.

The recoil fluence from a single collision and in the direction of s is then given by

$$F_s = \frac{\cos\theta}{\pi s^2} \tag{5}$$

The fluence in the direction of the incident neutrons is then

$$F_n = F_s \cos\theta$$

$$F_n = \frac{\cos^2\theta}{\pi s^2} \tag{6}$$

Finally, the differential response at P from the volume increment is

$$dR = dC \times F_n$$

$$dR = \frac{0.6025\rho\,\sigma\,dV}{A} \times \frac{\cos^2\theta}{\pi s^2}$$

Substituting for dV

$$dR = 1.205\rho\,\sigma \sin\theta \cos^2\theta\, d\theta\, ds/A \tag{7}$$

The analytical solution for the total response is then

$$R = \frac{1.205\rho\,\sigma}{A} \int_0^{\frac{\pi}{2}} \int_0^{s_{max}} \sin\theta \cos^2\theta\, d\theta\, ds.$$

After the first integration we have

$$R = \frac{1.205\rho\,\sigma}{A} \int_0^{\frac{\pi}{2}} s_{max} \sin\theta \cos^2\theta\, d\theta. \tag{8}$$

The quantity s_{max} is a complex function of θ. Physically, it is the maximum thickness of radiator material which a recoil particle, emitted at an angle, θ, to the incident neutron beam, can penetrate to produce a detectable track in the track recorder.

It can be seen that s_{max} is dependent upon initial recoil energy, E_r, and thus also upon scattering angle, θ, through the equation

$$E_r = \frac{4A\ E_n \cos^2 \theta}{(1+A)^2} \qquad (9)$$

where E_n is the neutron beam energy and A is the atomic number of the recoil nuclei. It is further dependent upon the following:

$R(E,Z_R)$, the range-energy relationship of the recoil ions in the radiator,

t_R, radiator thickness,

$R(E,Z_D)$, the range-energy relationship of the recoil ions in the degrader,

t_D, degrader thickness, and

ΔE_r, the effective minimum energy for production of detectable tracks in the track recorder.

For the neutron energies and recoil nuclei in question, it may be assumed that no upper limit on recoil energy exists for track registration. However, in order to be detected, a track must have some minimum length. This factor is responsible for the minimum energy, ΔE_r.

The substitution of an analytical expression for s_{max} in Equation 8, for completion of the integration, is obviously impractical. Instead, a numerical integration was done. In order for the numerical integration to closely approximate the analytical case, the integrand had to be calculated at intervals between the limits of integration which correspond to small changes in value. The value of s_{max} is at a maximum at $\theta = 0$ and decreases smoothly to zero at some angle less than $\theta = \pi/2$. Therefore calculations

at 1 degree intervals were considered sufficient.

Equation 8 can be replaced by

$$R = \frac{1.205\ K\ \rho\ \sigma}{A} \sum_{\theta=0}^{90} s_{max} \sin\theta \cos^2\theta. \qquad (10)$$

The quantity, K, is a factor necessary to renormalize the summation to the integral value. Since the original limits of integration were 0 to $\pi/2$, then for 90 intervals

$$K = (\pi/2 - 0)/90$$

$$K = 0.01745$$

Equation 10 then becomes

$$R = \frac{0.02103\rho\ \sigma}{A} \sum_{\theta=0}^{90} s_{max} \sin\theta \cos^2\theta\,. \qquad (11)$$

Since range-energy relationships are usually given in terms of mass thickness, mg/cm^2, it is convenient to use these units. The factor $10^{-3}/\rho$ converts mg/cm^2 to cm. Thus

$$R = \frac{2.103 \times 10^{-5}\ \sigma}{A} \sum_{\theta=0}^{90} s_{max} \sin\theta \cos^2\theta\,, \qquad (12)$$

and s_{max} is now to be calculated in units of mg/cm^2. Equation 12 holds only if the radiator is composed of a single element with a single isotope. Otherwise the two ρ's are not identical and

$$R = \frac{2.103 \times 10^{-5}\ \rho_1\ \sigma}{A\ \rho_2} \sum_{\theta=0}^{90} s_{max} \sin\theta \cos^2\theta \qquad (12\text{-b})$$

where ρ_1 is the density of the target nuclei within the radiator and ρ_2 is the total density of the radiator.

The summation and evaluation of Equation 12 was done with Program FLUENZ at a series of discrete neutron energies and for selected radiator materials and radiator and gold degrader thicknesses. The quantities

inputted to the program were A, atomic number of the scattered nuclei, a range-energy table for the radiator material and gold, called R(I), E(I), RA(I), the radiator and degrader thicknesses, called TR(I) and TD(I), the grid of neutron energies, called EF(I), and the target nuclei elastic scattering cross sections corresponding to the neutron energies, called SIGMA(I). Also a quantity called DELT was read in. This was a thickness of gold equal to the range of a recoil ion of energy ΔE_r, the minimum energy for production of a track in the plastic. By inputting DELT instead of ΔE_r, an extra range-energy interpolation was avoided, thus saving machine time.

In Program FLUENZ a nest of DO loops insured that the variables, EF, TR, TD, and θ are encountered in their proper order. First tables of $\cos\theta$, called B(N), and $\cos^2\theta$, called BTU(N), were calculated. Then, the elastically scattered recoil energy, called EE(J), is calculated according to Equation 9. Next, the recoil ion energy necessary to penetrate the degrader and register in the plastic is found. This quantity is interpolated from the range-energy table. It is the energy corresponding to gold thickness, DMAX, where

$$\text{DMAX} = \text{TD/B(J)} + \text{DELT}$$

and B(J) is $\cos\theta$. In the subroutine, the interpolated quantity is always called RANGE, whether it is, in fact, a range or an energy. Next, ranges in the radiator corresponding to recoil ions of two different energies are interpolated. One energy is that previously found, the minimum energy for penetrating the degrader and registering in the plastic. The other energy is EE(J). The second range minus the first is called BIT. Therefore, BIT is equal to the maximum range in the radiator which a recoil ion can span and still penetrate the degrader and register in the plastic.

The maximum thickness of the radiator, RMAX, is then found from

$$RMAX = TR/B(J).$$

If $RMAX \geq BIT$

then $S_{MAX} = BIT.$

If $RMAX < BIT$

then $S_{MAX} = RMAX.$

Thus, S_{MAX} is equal to the maximum possible recoil ion range for track registration unless this range is greater than the radiator thickness. In that case S_{MAX} is equal to radiator thickness. In the program S_{MAX} is called S. It is transferred into the subscripted variable, PATH(J), then multiplied by $\sin\theta\cos^2\theta$ and summed over the 90 angular intervals as in Equation 12. After the summation, Equation 12 is completed by a multiplication by the proper factor. The product is stored for printout as FLU(I,K,L). The subscripts correspond to the values selected for EF(I), TR(K), and TD(L).

For EF(I), a grid of 40 neutron energies, separated by 0.5 MeV and extending to 20 MeV, was employed. The corresponding elastic scattering cross sections used were averaged over 0.5 MeV intervals about the neutron energies. The calculated detector responses should therefore be considered histograms summed over the same energy intervals rather than true differential responses. The cross sections of ^{9}Be, ^{12}C and ^{16}O collected for this purpose[5,6] are given in Table 2. Some gaps occurred in available data, especially above 15 MeV, and extrapolations or interpolations were made to fill in the regions. The values of TR(K) and TD(L) were those of actual detectors such as are given in Table 1. The value of ΔE_r was taken to be 0.36 MeV. This value is difficult to determine exactly from observations of tracks due to recoils of mixed energies. It will be fixed, finally,

TABLE 2

Interval-Average (0.5 MeV) Elastic Scattering Cross Sections Used In Program FLUENZ. The Units Are barns.

Neutron Energy (MeV)	^{9}Be	^{12}C	^{16}O
0.5	4.2	-	-
1.0	3.6	-	-
1.5	2.26	2.20	3.15
2.0	1.85	1.71	1.82
2.5	2.23	1.60	0.880
3.0	2.87	1.873	1.488
3.5	1.76	2.138	2.995
4.0	1.38	2.000	2.350
4.5	1.22	1.689	1.537
5.0	1.165	1.288	1.249
5.5	1.120	1.044	1.426
6.0	1.080	0.939	1.400
6.5	1.050	0.880	1.081
7.0	1.027	0.529	1.449
7.5	1.010	1.150	1.043
8.0	1.000	1.340	0.837
8.5	0.995	1.000	0.689
9.0	0.990	0.786	0.575
9.5	0.985	0.705	0.477
10.0	0.980	0.695	0.534
10.5	0.976	0.755	0.584
11.0	0.971	0.810	0.628
11.5	0.966	0.823	0.665
12.0	0.961	0.818	0.700
12.5	0.956	0.812	0.733
13.0	0.952	0.804	0.748
13.5	0.947	0.797	0.744
14.0	0.942	0.788	0.738
14.5	0.937	0.780	0.729
15.0	0.933	0.773	0.722
15.5	0.928	0.766	0.715
16.0	0.923	0.759	0.709
16.5	0.918	0.752	0.703
17.0	0.913	0.745	0.698
17.5	0.909	0.739	0.693
18.0	0.904	0.733	0.688
18.5	0.899	0.727	0.683
19.0	0.894	0.722	0.67[illegible]
19.5	0.889	0.717	0.675
20.0	0.885	0.712	0.671

by comparing calculations of detector response with experimental measurement. The range-energy tables for ions in radiator and degrader materials were taken from Northcliffe and Schilling.[7]

Figures 2 and 3 show the results of calculations for the beryllium radiators and gold degraders given in Table 1. Rather than present histograms, smooth curves have been drawn through neutron energy grid points. A listing of the program is given in Appendix A.

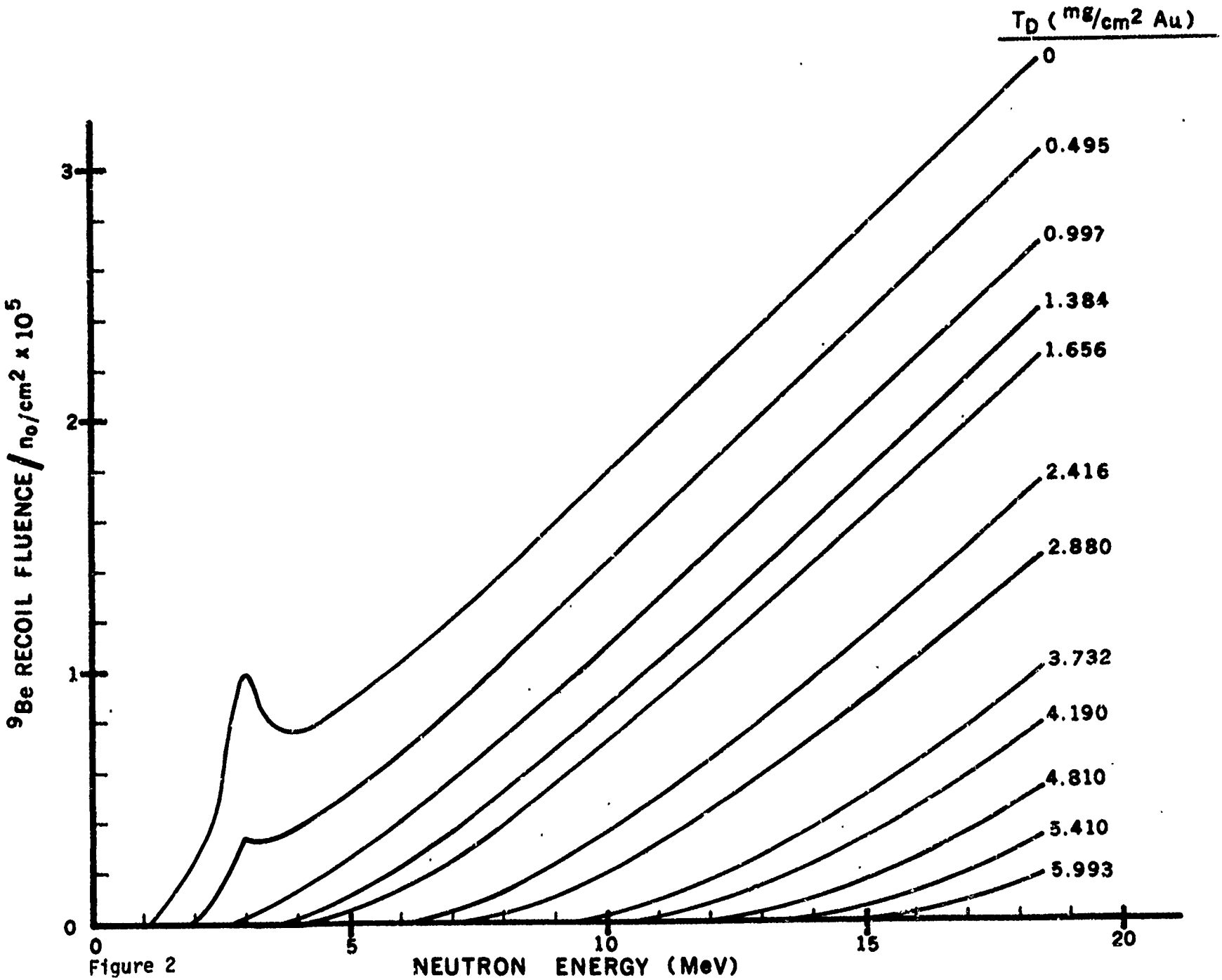
T_D (mg/cm2 Au)
0
0.495
0.997
1.384
1.656
2.416
2.880
3.732
4.190
4.810
5.410
5.993
^{9}Be RECOIL FLUENCE/n_o/cm^2 x 10^5
0
1
2
3
0
5
10
15
20
NEUTRON ENERGY (MeV)

Figure 2

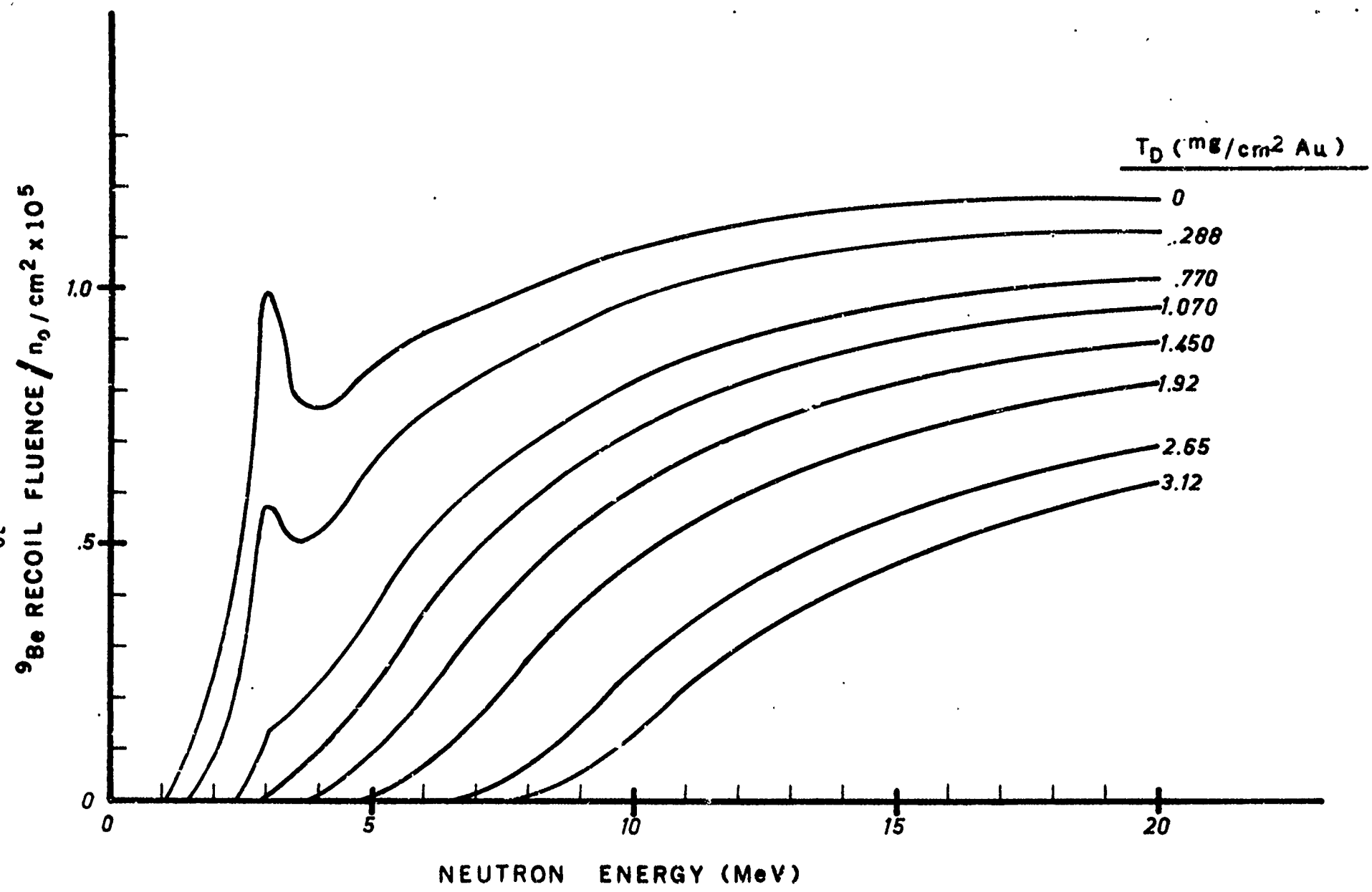
T_D (mg/cm² Au)
0
.288
.770
1.070
1.450
1.92
2.65
3.12
^{9}Be RECOIL FLUENCE / n_o / cm² x 10⁵
1.0
.5
0
0
5
10
15
20
NEUTRON ENERGY (MeV)

Figure 3

IV. Spectral Unfolding

The development of a computerized unfolding program to obtain neutron spectra from HEND measurements, Program HENDU, is in progress. The unfolding employs an iterative technique similar to the SAND Program of McElroy, et. al.[8] The SAND unfolds activation foil measurements into neutron spectra. It employs a set of activation foils with overlapping responses (interaction cross sections) covering the desired neutron energy range.

An inspection of the problem reveals the basis for the unfolding. Any discrete neutron spectrum will be sampled by each activation foil, according to the cross section, to yield a set of measured activations. A model spectrum is then folded into each cross section curve to yield a corresponding set of calculated activations. A comparison of the calculated and the measured activations gives information on how the model spectrum should be changed to approximate the experimental spectrum. In practice an iterative scheme generates successive approximations to the experimental neutron spectrum until a "best fit" is found for the activation measurements. If there were no significant errors present in either the cross sections or experimental activation measurements, and if the neutron energy range were well covered by overlapping activation foil cross section peaks, then this method would yield excellent results. In practice, fairly good results are obtained over wide energy regions (±10 to ±30% by McElroy).

The least reliable of McElroy's measurements tend to be at the higher neutron energies. There are few well placed interactions of high cross section with proper decay times in this region. Therefore, the HEND system should yield better results within its region or applicability (~5 to 20 MeV) than do activation foils.

A summary of Program HENDU follows. The series of detector response curves may be thought of as a matrix, R(I,J), where I denotes the detector grid and J the neutron energy grid. Each detector yields a measurement of track density, A, and the series of track densities may be denoted A(I). The neutron energy grid consists of intervals 0.5 MeV wide. The interval center energies are denoted

by E(J).

Another array quantity necessary as input to the unfolding program is the first approximation neutron spectrum. The first approximation should be as close to the actual experimental spectrum as possible. The solutions to iterative fitting programs such as HEPDU are non-unique and, in general, the less "work" necessary to gain a fit to the experimental spectrum, the better that fit will be. This first approximation, CALC(J), which is either calculated or selected by other means, will initially be inputted to the program in tabular form.

The program can be outlined with the following quantities:

A(I)

E(J)

R(I,J)

CALC(J)

IMAX, the total number of detectors used,

JMAX, the total number of energy intervals, and

KMAX, the maximum number of iterations allowed.

The iterative portion of the program begins with

$$AC(I) = \sum_{J=1}^{JMAX} CALC(J)*R(I,J) \qquad (13)$$

where AC(I) are the calculated track densities corresponding to the measured track densities A(I). In fact, if CALC(J) is equal to the actual experimental neutron spectrum, then within the statistics of the measurements, AC(I)=A(I).

CALC(J) and AC(I) are then normalized to the measurements. That is

$$CALC(J) = CALC(J)* \sum_{I=1}^{IMAX} A(I)/[AC(I)*IMAX] \qquad (14)$$

$$AC(I,J) = CALC(J)*R(I,J), \text{ and} \tag{15}$$

$$AC(I) = \sum_{J=1}^{JMAX} AC(I,J) \tag{16}$$

Since these quantities are recalculated over and over again by the iterative cycle, they can be ranked according to iteration number, K, for better understanding of the procedure. Thus, the initial approximation spectrum may be labeled $CALC(J)^{[0]}$ and calculated track densities $AC(I)^{[0]}$ since no iterations have yet occurred.

Next the quantities $DEV(I)^{[0]}$ and $STDV^{[0]}$ are calculated. DEV(I) are the individual deviations of the ratio of measured to calculated track densities for each detector from the average ratio, in absolute fraction. This is

$$DEV(I) = \left(\frac{A(I)}{AC(I)}\right) / \left(\left(\sum_{I=1}^{IMAX} \frac{A(I)}{AC(I)}\right) / IMAX\right) - 1. \tag{17}$$

STDV is the current iterative value of the standard deviation of all the DEV(I). Thus

$$STDV^{[k]} = SQRT\left(\sum_{I=1}^{IMAX} DEV(I)^{[k]} **2 / (IMAX-1)\right). \tag{18}$$

The weighting factors, WATE (J), are then calculated. The first approximation spectrum is transformed into the first iterative spectrum by

$$CALC(J)^{[1]} = CALC(J)^{[0]} * EXP\ (WATE(J)^{[0]}). \tag{19}$$

for the $K^{\underline{th}}$ iteration

$$WATE(J)^{[k]} = \frac{\sum_{I=1}^{IMAX} W(I,J)^{[k]} \ln\left(\frac{A(I)}{AC(I)^{[k]}}\right)}{\sum_{I=1}^{IMAX} W(I,J)^{[k]}} \quad \text{where:} \tag{20}$$

$$W(I,J)^{[k]} \equiv \frac{AC(I,J)^{[k]}}{AC(I)^{[k]}} \qquad (21)$$

In the calculation of WATE(J), the values of A(I) cannot be allowed to equal zero, since ln 0 = - ∞. Ambiguous values of DEV(I) and STDV would also be obtained for this condition. Experimentally these values can equal zero. For these calculations, an arbitrarily small value, 1×10^{-4}, is substituted for any zeros.

$CALC(J)^{[1]}$ is then transferred back into Equation 1 and the second iteration begins. The iteration number, K, is set up to keep a running score of how many iterations have taken place. When KMAX is reached, the program is terminated. Another method of terminating the program is by comparisons of STDV for successive iterations. A knowledge of counting statistics allows one to calculate the statistical errors associated with A(I). From these an expected standard deviation, XSTD, can be calculated and inputted to the program. When STDV = XSTD, then a fit has been found to the experimental neutron spectrum. In either case, a listing is made of DEV(I) and STDV for every iteration. This allows any serious errors in measurements to be recognized and a record of convergence to be examined.

Program HENDU, as developed to date, is given in Appendix B. Some additional quantities have been added for practical reasons. A table of definitions precedes to program.

Up to the present time Program HENDU has been tested with a response matrix R (I,J), composed of several response curves of the thick radiator type. Simple model spectra have been unfolded. The unfolding took place in a generally satisfactory manner. With few detectors having widely spaced neutron energy thresholds, and beginning with a flat first approximation spectrum, the unfolded spectrum tends to fit the model spectrum in segments corresponding to the interthreshold gaps. Figure 4 demonstrates

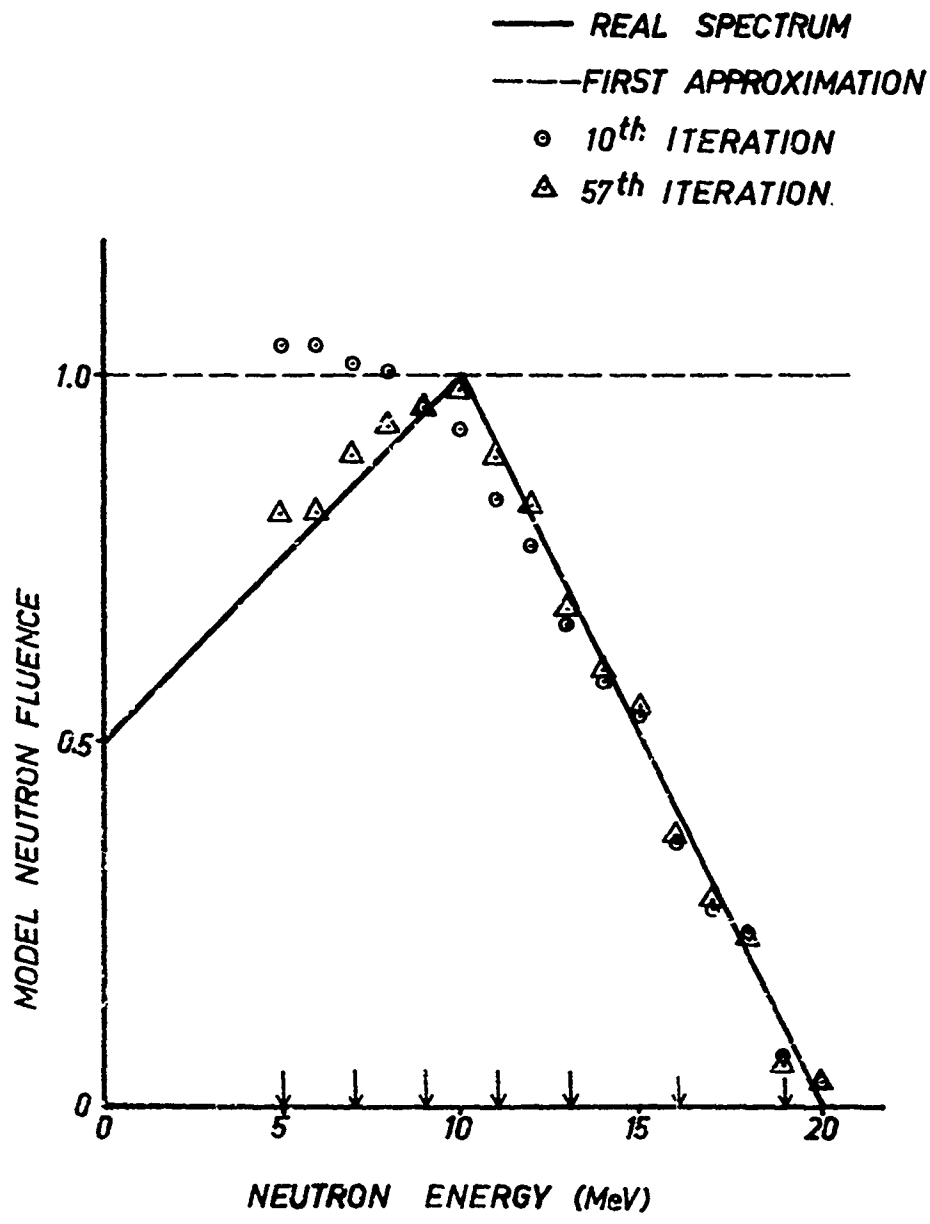
REAL SPECTRUM
FIRST APPROXIMATION
10th ITERATION
57th ITERATION
1.0
0.5
0
MODEL NEUTRON FLUENCE
0
5
10
15
20
NEUTRON ENERGY (MeV)

Figure 4

one such unfolding. The arrows at the bottom denote the first values of each of the seven response curves. The first response begins at 5 MeV. The unfolded spectrum can extend down in energy only this far. The high energy part of the spectrum, which was well sampled by the responses, converged rather rapidly. At low energies, where sampling was meager, convergence was much slower. One method of improving the situation is to add detectors whose responses are not peaked so heavily toward higher energies. Thin radiator responses, such as those in Figure 3, have this property. Also, the thresholds, instead of being rather evenly spaced, can be shifted toward lower energies. The optimum number of detectors will be decided from tests under experimental circumstances and including statistical counting errors.

V. Applications

The HENRD system can be applied to the spectral measurement of high energy neutrons over a rather wide range of fluences. The saturation fluence with beryllium radiators is about 10^{11} n_0/cm^2, although detectors with the more sensitive responses may begin to saturate at smaller values. This range can be extended by using thin polyethylene radiators. The smaller probability of emitting ^{12}C recoils from these radiators increases the saturation fluence to about 5×10^{11} n_0/cm^2. At this fluence, background track densities, due to recoil events occurring within the track recorder, become very significant. It is necessary to count large numbers of tracks to reduce statistical errors in the measurements. Consequently, manual counting becomes too laborious to undertake.

The lowest detectable fluence depends on both the energy spectrum of the neutrons and the particular detector configuration in question. For the more sensitive detectors with beryllium radiators, the average sensitivity is about 1.5×10^{-5} tracks/neutron, as seen from Figure 2. A fluence of 1.5×10^{8} n_0/cm^2 would yield 10^3 tracks/cm^2. This is a low density for counting recoil tracks. At present, even the best of plastic track recorders contain background pits whose density is a substantial fraction of this number. In addition, manual counting of such densities is time consuming if statistical errors are to be kept low.

The effective neutron energy range of the detector is about 5 to 20 MeV. Below 5 MeV efficiencies become quite low for the most sensitive detector configurations. Neutron energies above 20 MeV will certainly produce tracks, but the response in this region can no longer be described by a simple elastic scattering procedure.

Methods for automatic counting of tracks have been used[9,10] or are

being developed[11,12]. For the most part these were developed for counting of fission fragment tracks, but the same methods can also be applied to counting of recoil tracks. The adaptation of an automatic counting technique would greatly facilitate the use of these detectors at all fluence ranges.

To summarize, some of the advantages of the HEND system are: (1) small size ($\sim$1 cm^2) and light weight (a few grams), (2) stability (track registration characteristics of nuclear track detectors remain constant over long periods of time), (3) permanently recorded tracks (can be read any time following exposure), (4) insensitivity to X- or gamma-ray backgrounds below $\sim 10^6$ rads, (5) absense of flux effects (very high intensity pulses of neutrons can be measured without detector response fluctuations), (6) independence of reaction half-life constraints, and (7) wide neutron energy range coverage (cross sections exist for threshold measurements of neutrons with energies between $\sim$5 and 20 MeV). The detectors are passive devices but active readout could probably be attained.

VI. Conclusions

At this time, the configuration of the detector has been established and the type of information to be gained from their use is well understood. The ability of the system to yield useful spectral information is indicated.

A lengthy but necessary development of a special track recorder for efficient, selective registration of recoil particles has been completed. This was achieved by reducing the sensitivity of a cellulose nitrate plastic below the registration threshold of ^{4}He particles. Calibration measurements can now proceed with the final version of the detectors.

A calculational method of determining neutron energy response of the detectors has been completed. Experimental verification at a few energies will validate the calculations.

A spectral unfolding program has been developed. It has been shown to yield model spectra for situations similar to the experimental conditions.

VII. Appendices

Programs FLUENZ and HENDU were written in Fortran IV. They were run on a Univac Series 70 (formerly RCA Spectra 70) computer. This machine is not comparable in speed to those generally encountered for scientific application. The programs ran for about 280 and 170 seconds, respectively.

A. Program FLUENZ

Main program: reads and writes all input data deck cards and writes output, controls program flow; calculates recoil particle fluence leading to production of tracks in nuclear track detector for a given set of detector parameters.

Subroutine NTERP: performs interpolations on range-energy tables of energetic ions in selected media (selects either range from energy or energy from range).

The program variables are:

A,	atomic number of the recoil,
DELT,	a range in gold corresponding to the minimum energy of the recoil nuclei for track registration,
R(N), E(N), RA(N),	range-energy table for the recoil nuclei in the radiator and gold degrader,
EF(I),	the neutron energies (MeV).
SIGMA(I)	elastic scattering cross sections
TD(J),	degrader mass thicknesses (mg/cm^2),
TR(K),	radiator mass thicknesses (mg/cm^2),
B(90),	$\cos\theta$ at 1 degree intervals,
BTU(90),	$\cos^2\theta$ at 1 degree intervals,
EE(90),	recoil nuclei energies versus θ
FLU(I,K,L),	calculated track-producing recoil fluences,
PATH(90),	intermediate step for summing FLU over θ.

```
1          Program FLUENZ
2          DIMENSION FLU (40,12,2), EE(90), PATH(90), B(90), BTU(90)
3          DIMENSION R(23), E(23), RA(23), TR(2), TD(12), EF(40),
             SIGMA(40)
4          READ (5,11) A,DELT
5  11      FORMAT(2F10.3)
```

```
 6                READ (5,12) ((R(I),E(I),RA(I)),I=1,23)
 7  12            FORMAT (3F10.4)
 8                READ (5,15) (TR(I),I=1,2)
 9                READ (5,15)(TD(I),I=1,8)
10                READ (5,15)(EF(I), I=1,40)
11                READ(5,15)(SIGMA(I),I=1,40)
12  15            FORMAT (8F10.3)
13                WRITE (6,18) A,DELT
14  18            FORMAT (1H0,2F6.3)
15                WRITE (6,17) ((I,R(I),E(I),RA(I)),I=1,23
16  17            FORMAT (1H ,I5,3F8.4)
17                WRITE (6,19) (TR(I),I=1,2)
18                WRITE (6,19) TD(I),I=1,8)
19  19            FORMAT (1H ,F7.3)
20                WRITE (6,16) ((I,EF(I).SIGMA(I)),I=1,40)
21  16            FORMAT (1H ,I5,2F7.3)
22                DO 5 N=1,90
23                B(N)=COS((N-1.)*.0174533
24  5             BTU(N)=B(N)*B(N)
25                DO 210 I=1,40
26                X=4.*A*EF(I)/((1.+A)*(1.+A))
27                DO 210 K=1,8
28                DO 210 L=2,2
29                DO 200 J=2,90
30                EE(J)=X*BTU(J)
31  C                   EFFECT OF DEGRADER THICKNESS
32                DMAX=(TD(K)/B(J))+DELT
33                IF(DMAX.GT.9.797) GO TO 121
34  C               9.797 (MG/SQ CM) IS MAX VALUE IN INTERP TABLE FOR BE ON AU
```

```
35  50          CALL NTERP (E,RA,DMAX, RANGE)
36  C           'RANGE' IS NOW THE MIN. ENERGY ION THAT CAN PENETRATE DEGRADER
37  C           AND REGISTER IN PLASTIC
38              TEST=RANGE
39              CALL NTERP (R,E,TEST,RANGE)
40              RANGE1=RANGE
41              CALL NTERP (R,E,EE(J),RANGE)
42              BIT=RANGE-RANGE1
43              IF(BIT.GT.0.) GO TO 401
44              GO TO 121
45  C                 EFFECT OF RADIATOR THICKNESS
46  401         RMAX=TR(L)/B(J)
47              IF (RMAX-BIT)101,101, 102
48  C              S IS SET TO EITHER RMAX OR BIT, WHICHEVER IS SMALLER
49  101         S = RMAX
50              GO TO 103
51  102         S=BIT
52  103         CONTINUE
53              PATH(J)=S
54              PATH1=PATH(J)
55              IF(PATH(J).LE.0.) GO TO 121
56              PATH(J)=PATH(J)*SIGMA(I)*SQRT(1.-BTU(J))*BTU(J)
57  200         CONTINUE
58  C                 SUMMATION OVER ALL ANGLES
59  121         JMAX=J-1
60              IF(JMAX.LT.2) GO TO 203
61              DO 202 M=2,JMAX
62  202         PATH(M)=PATH(M) + PATH(M-1)
```

```
63                      GO TO 209
64  203                 PATH(JMAX)=0.
65  209                 FLU(I,K,L)=2.33E-6*PATH(JMAX)
66  210                 CONTINUE
67                      WRITE (6,21)
68 21                   FORMAT (1HO)
69                      DO 211 L=2,2
70                      WRITE (6,13)A,TR(L)
71  13                  FORMAT (1H1,'MASS NUMBER' , F4.0,'/' , F6.3,' MG/CM**2')
72                      DO 211 K=1,8
73                      WRITE (6,22)
74  22                  FORMAT (1HO,'   DEGRADER    ENERGY   FLUENCE');
75                      DO 211 I=1,40
76                      WRITE (6,14) L,K,I,TD(K),EF(I),FLU(I,K,L)
77  14                  FORMAT (1H , 315,2F8.3,E14.6)
78  211                 CONTINUE
79                      STOP
80                      END
81                      SUBROUTINE NTERP (DIST,ENER,EION,RANGE)
82                      DIMENSION DIST(23),ENER(23)
83                      J=1
84  300                 IF (EION-ENER(J))301,302,303
85  301                 RMAX=DIST(J)
86                      EMAX=ENER(J)
87                      GO TO 304
88  302                 RANGE=DIST(J)
89                      GO TO 309
90  303                 RMIN=DIST(J)
```

```
 91                EMIN=ENER(J)
 92                J=J+1
 93                GO TO 300
 94  304           CONTINUE
 95                IF(EMAX-EMIN)305,305,306
 96  305           RANGE=0.
 97                GO TO 309
 98 306           RANGE=RMIN+(((RMAX-RMIN)*(EION-EMIN))/(EMAX-EMIN))
 99  309           CONTINUE
100                RETURN
101                END
```

B. Program HENDU

Input:

Card No.	Format	Quantity	Interpretation
1	5I5	KTRL(L), L=1,5	KTRL(1)=0 Given values of A(I) are read in.
			KTRL(1)>0 A(I) are computed using a known spectrum.
			KTRL(2)=0 No graph is plotted
			KTRL(2)=1 Final iteration is plotted.
			KTRL(2),L>2 No assignment has been given to these values yet and thus they can be used as control cards in the future use of the program.
2	3I5,F10.3	KMAX	# of iterations
		IMAX	# of targets
		JMAX	# of energy points
		EMAX	Maximum energy, i.e.,EMAX=E(JMAX) in general $E(J)=\frac{EMAX}{JMAX} \times J$.
3	9F8.3	CALC(J),J=1,JMAX	Value of initial approximation spectrum at energy points E(J).
4	16I5	START(I),I=1,IMAX	First J value for which R(I,J) is to be given for each I. It is assumed that R(I,J)=0 for all J≤ START(I).
5	4(F10.5,10x	R(I,J),J=1,JMAX	For each I value, the value of the response curves R(I,J) for each point J from START(I) to JMAX.
6	a) KTRL(1)>0 9F8.5	TH(J),J=1,JMAX	Value of theoretical true spectrum at energy values E(J).
	b) KTRL(1)=0 9F8.3	A(I),I=1,IMAX	Track densities corresponding to R(I,J).

Output:

1. Value of R(I,J) for each I in ascending order of J. No title given.

2. Values of A(I). These are only given if they were computed from theoretical curve, i.e., if KTRL(1)>0 (title given).

3. Iteration number starting at KMAX-5 (title given).

   i) Standard deviation (with title).

   ii) The value of CALC(J) for each J, i.e., the value of the computed spectrum at each J value (with title).

   iii) The value of AC(I) for each I, i.e., the iterated values of the track densities.

4. If KTRL(2) = 1
   For each value of J a point is plotted giving the value of the final iterated spectrum. A smooth curve of the initial theoretical spectrum is also given.
   N.B. As yet no consideration has been given to the use of KTRL(1)=0 in which case the smooth curve would have no meaning. Modifications are still needed to be made to the program to exclude the smooth curve when KTRL(1)=0.

```
1                 PROGRAM HENDU
2                 COMMON  A(20),R(20,40)
3                 COMMON  TH(42),CALC(42),E(42)
4                 DIMENSION KTRL(5),AC(20)
5                 INTEGER START(20)
6                 READ(5,16) (KTRL(L),L=1,5)
7                 READ(5,13) KMAX, IMAX, JMAX, EMAX
8                 READ(5,14) CALC(J), J=1,JMAX)
9                 READ (5,72) START (K), I=1,IMAX)
10                DO 15 I=1,IMAX
11                JMIN=START(I)
12                JJ=JMIN-1
13                DO 70 J=1,JJ
14  70            R(I,J) = 0.0
```

```
15  15          READ (5,71) (R(I,J), J=JMIN, JMAX)
16              DO 80 I=1,IMAX
17              DO 81 J=1,JMAX
18  81          R(I,J)=R(I,J)*10**3
19  80          CONTINUE
20              DO 73 I=1,IMAX
21  73          WRITE(6,14) (R(I,J), J=1,JMAX)
22              IF (KTRL(1)) 18,18, 17
23  17          READ (5,57) (TH(J),J=1,JMAX)
24              DO 31 I=1,IMAX
25              DO 32 J=1,JMAX
26              IF (R(I,J)-0.0)32,32,33
27  33          A(I)=A(I)+TH(J)*R(I,J)
28  32          CONTINUE
29  31          CONTINUE
30              GO TO 19
31  18          READ (5,14) (A(I),I=1,IMAX)
32  19          WRITE (6,35)
33              WRITE (6,12) (A(I),I=1,IMAX)
34              DO 47 J=1,JMAX
35  47          E(J)=EMAX/JMAX*J
36  C           CALCULATION OF F
37              K=0
38  200         F=0
39              DO 100 I=1, IMAX
40  100         AC(I)=0.0
41              DO 101 I=1,IMAX
42              DO 102 J=1,JMAX
```

```
43  102         AC(I)=AC(I)+CALC(J)*R(I,J)
44              IF(AC(I))  101,101,120
45  120         F=F+A(I)/AC(I)
46  101         CONTINUE
47              F=F/IMAX
48  C           NORMALIZING INPUTS
49              DO 103 I=1,IMAX
50  103         AC(I)=AC(I)*F
51              DO 104 J=1,JMAX
52  104         CALC(J)=CALC(J)*F
53  C           COMPUTE STD DEV
54              STD=0
55              DO 108 I=1, IMAX
56              DEV=A(I)/(AC(I)*F)-1
57  108         STD=STD+DEV**2
58              STDV=SQRT  (STD/(IMAX-1))
59              L=KMAX-5
60              IF (L-K) 202,202,203
61  202         WRITE (6,10) K,STDV
62              WRITE(6,11)
63              WRITE(6,12) (CALC(J), J=1,JMAX)
64              WRITE(6,12)  (AC(I), I=1,IMAX
65  203         K=K+1
66              IF(K-KMAX) 201,201,900
67  C  CALCULATION OF WEIGHT FACTORS
68     201      DO 106 J=1, JMAX
69              DEN=0
70              TUM=0
```

```
71                DO 107 I=1, IMAX
72                IF(AC(I)-.0001) 107,107,109
73   109          W=CALC(J)*R(I,J)/AC(I)
74                DEN=DEN+W
75                TUM=TUM+W*ALOG(A(I)/AC(I))
76   107          CONTINUE
77                IF (DEN-.00001) 110,110,111
78   110          WATE=0.0
79                GO TO 106
80   111          WATE=TUM/DEN
81   106          CALC(J)=CALC(J)*EXP(WATE)
82                GO TO 200
83   10           FORMAT(/12H ITER. STEP=,13,10X,5HSTDV=,F10.3)
84   11           FORMAT(10X,7HCALC(J))
85   12           FORMAT( 5F15.3)
86   13           FORMAT( I5,F10.3)
87   14           FORMAT( 9F8.3)
88 16             FORMAT(5I5)
89   71           FORMAT(4(F10.5,10X))
90   72           FORMAT(10I5)
91   900          IF(KTRL(2))901,902,901
92   901          CALL GRAPH
93   902          STOP
95                END

96                SUBROUTINE GRAPH
97                COMMON IMAX, JMAX, A(20),R(20,40)
```

```
      COMMON TH(42),CALC(42),E(42)
      DIMENSION IBUF(1000)
      CALL PLOTS(IBUF,1000,8)
      CALL PINIT('H200','117',20,'CALCULATED SPECTRUM')
      CALL PLOT(0 0,0.75,-3)
      I1=JMAX+1
      I2=JMAX+2
      CALL SCALE(E,10.0,JMAX,1)
      CALL SCALE(TH,5.0,JMAX,1)
      CALL AXIS(0.0,0.0,13HENERGY IN MEV,-13,10.0,0.0,E(I1),E(I2))
      CALL AXIS(0.0,0.0 ,8HSPECTRUM,8,5.0,90.0,TH(I1),TH(I2))
      CALC(I1)=TH(I1)
      CALC(I2)=TH(12)
      CALLFLINE(E,TH,JMAX,1,0,0)
      CALL LINE(E,CALC,JMAX,L,-1,2)
      CALL PLOT(15.0,-0.5,999)
      RETURN
      END
```

VIII. References

1. W. N. McElroy, Activation Foil Spectrometry - Energies Less Than 14 MeV, ANS Transactions, 13, No. 1, June 1970.

2. R. C. Barrall, Activation Foil Spectrometry - Energies Near 14 MeV, ANS Transactions, 13, No. 1, June 1970.

3. A. L. Frank and E. V. Benton, "Neutron and Gamma-Ray Measurements With Nuclear Track Detectors," DASA No. 2573, (30 November 1970).

4. E V. Benton, "A Study of Charged Particle Tracks in Cellulose Nitrate," USNRDL-TR-68-14, (22 January 1968).

5. 'Neutron Cross Sections,' BNL 325 (Second Ed., Suppl. 2), Vol. I, (May 1964).

6. J. Adir, A. S. Clark, R. Froelich, L. J. Todt, "'Users and Programmers' Manual for the GGC-3 Multigroup Cross Section Code." Part 1 (Users's Part), GA-7157 (7-25-67).

7. L. C. Northcliffe and R. F. Schilling, Nuclear Data 7, Nos. 3,4 (1970).

8. W. N. McElroy, S. Berg, T. Crockett, R. G. Hawkins, "A Computer-Automated Iterative Method for Neutron Flux Spectra Determination By Foil Activation," AFWL-TR-67-41, Vols. I-IV, (Sept. 1967).

9. N. G. Cross and L. Tommasino, Proc. International Topical Conference on Nuclear Track Registration in Insulating Solids and Application (University of Clermont, Clermont-Ferrand, France, 1969) Vol. 1, p. 73.

10. D. Jowitt, "Nuclear Instruments and Methods," 92, 37 (1971).

11. C. E. Cohn and R. Gold, "Review of Scientific Instruments," 43, 12, (1972).

12. R. Gold and C. E. Cohn, "Review of Scientific Instruments," 43, 18, (1972).